

1
2
3
4
5
6
7
8
9
10
11
12
13
14
15
16
17

The Flux Monitor (Technical Note)

M. Bashkanov,* D. P. Watts, and N. Zachariou
Department of Physics, University of York, Heslington, York, Y010 5DD, UK

E. Chudakov and H. Egıyan
Thomas Jefferson National Accelerator Facility, Newport News, VA 23606, USA

M. Amaryan
Old Dominion University, Norfolk, VA 23529, USA

S. Dobbs
Florida State University, Tallahassee, FL 32306-4350, USA

J. Ritman
Institut für Experimentalphysik I - Ruhr-Universität, Bochum 44780, Germany

J. R. Stevens
College of William and Mary, Williamsburg, VA 23185, USA

I. Strakovsky
The George Washington University, Washington, DC 20052, USA
(Dated: July 1, 2023)



* mikhail.bashkanov@york.ac.uk

CONTENTS

18

19	I. K_L Flux Monitoring	3
20	II. Flux Monitor Location	3
21	III. Acceptance and Dimensions of the Flux Monitor	3
22	IV. K_L Flux Determination	7
23	V. Vertex Position Reconstruction	8
24	VI. Decay Reconstruction	9
25	A. Background	11
26	VII. Neutron Background	11
27	VIII. Online Monitoring	12
28	IX. Existing Equipment and Relocation Timeline	12
29	X. Decommissioning	13
30	XI. Costs	13
31	XII. JLab Contribution	13
32	XIII. Summary	13
33	XIV. Appendix A: CAD Drawings	14
34	References	17

Abstract. An accurate determination of the K_L beam flux is necessary to maximise the physics impact of the resulting data. During proposal stage several versions of the Flux Monitor (KFM) were considered. We have finally agreed on a least risky and the most affordable design with ability to extend/upgrade it further at any stage if finances permits. Current design allows to reconstruct Kaon beam flux with accuracy of 5% over all momentum range. For the hyperon spectroscopy beam momentum range, the flux determination statistical accuracy of better than 1% is achievable within a day.

I. K_L FLUX MONITORING

An accurate determination of the K_L beam flux is necessary to maximise the physics impact of the resulting data. To reach an accuracy of $< 5\%$ in the determination of the K_L flux we plan to build a dedicated Flux Monitor (KFM). This will provide a significant improvement over the typical 10% accuracy achievable from normalisation of the data to previously measured reactions, for instance, $K_L p \rightarrow K_S p$.

The operation of a KFM could employ the regeneration of K_S and detection of $\pi^+\pi^-$ pairs in Pair Spectrometer as done at Daresbury [1]. However, this technique affects the quality of the resulting K_L beam. Therefore, a more effective choice for the KFM at JLab would utilise in-flight decays of the K_L . The K_L has four dominant decay modes [2]:

- $K_L \rightarrow \pi^+\pi^-\pi^0$ BR = 12.54% .
- $K_L \rightarrow \pi^0\pi^0\pi^0$ BR = 19.52% .
- $K_L \rightarrow \pi^\pm e^\mp \nu$ BR = 40.55% .
- $K_L \rightarrow \pi^\pm \mu^\mp \nu$ BR = 27.04% .

All decay modes with two charged particles in the final state can be used for flux determination. However, in this memo we will concentrate on a simplest one $K_L \rightarrow \pi^+\pi^-\pi^0$ where both charged particles have the same mass.

II. FLUX MONITOR LOCATION

To account for various possible acceptance effects during K_L beam propagation from the Be target, we plan to measure the K_L flux upstream of the GlueX detector, utilising the Hall D Pair Spectrometer as a shielding against K_L which have decayed further upstream. As seen from the Figure 1, our current design of the KFM fits downstream the Glue-X pair spectrometer magnet very well. The only equipment which needs to be dismount prior to installation of KFM is a pair spectrometer with a shielding wall.

III. ACCEPTANCE AND DIMENSIONS OF THE FLUX MONITOR

All the K_L decay products are very forward peaked, but one needs to have sizeable detectors to reconstruct K_L distributed along the length of the 24 m beamline. The FM design proposed and described in this memo will measure a small fraction of decayed K_L 's, concentrating on the portion decaying within a distance of 2 m downstream of the pair spectrometer magnet centre, Fig. 1. To fulfil this requirement a detector system of roughly 50 cm diameter is sufficient, however, since we will reutilise existing components, we will cover much larger range, namely 75 cm diameter at the ‘‘Start station,’’ ~ 2.5 m diameter at ‘‘Stop station’’ and 70 cm bore of an optional MRI magnet. On Figure 2 one can see an acceptance for a 70 cm diameter system for various decay branches as a function of K_L beam momentum.

Figure 2 shows the achievable acceptance for flux monitor based on an endcap designs. The 3π branch has sizeable and reasonably uniform acceptance over the full range of K_L . The flux monitor described in this memo consists of the following major parts: the Start detector (Fig. 3), the forward tracker, the backward tracker (Fig. 5), the Stop detector (Fig. 4) and an optional solenoid magnet from used MRI (Fig. 7).

The Start detector is a pizza-piece shaped segmented double-layer plastic scintillator, a former WASA-at-COSY Forward Proportional Chamber used to provide start timing signals for time-of-flight (ToF) as well as signals for the trigger electronics. Each layer has 24 elements and is built of 3 mm thick BC408 plastic scintillator coupled to XP1312 PMT from Phosics with twisted adiabatic lightguides. All PMT's are housed in individual μ -metal cylinders to shield from magnetic field. Further details can be found in Ref. [3]. Dimensions of the supporting structures are also shown

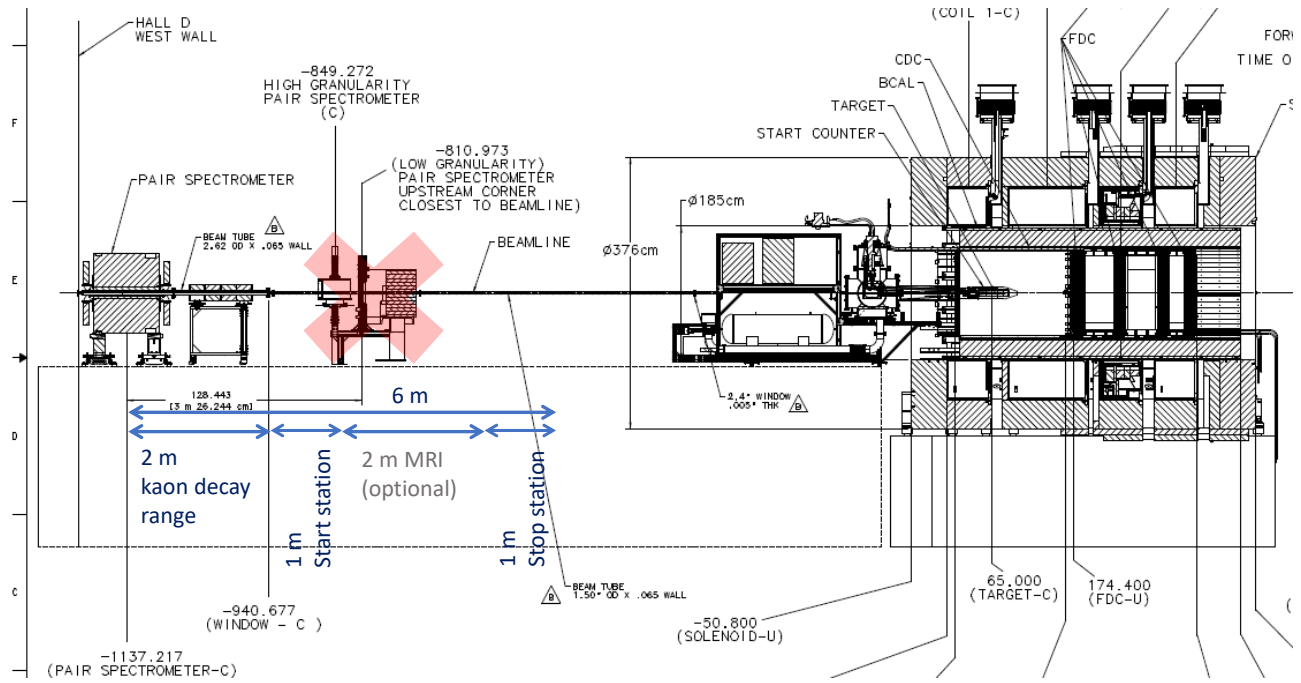


FIG. 1. The Flux Monitor Location in a Hall D. The red cross pointed to the pair spectrometer, which needs to be removed prior to KFM installation.

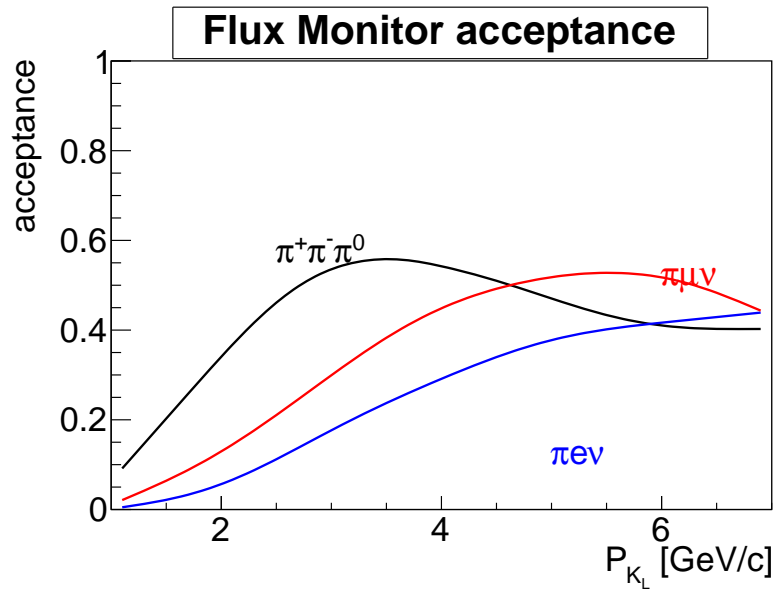


FIG. 2. The Flux monitor acceptance for various decay branches.

80 in Appendix A. A detector is available for collection from Q4 2023. The detector has 75 cm diameter active area and
 81 0.16 ns time resolution [3] which exceed the KFM requirement.

82 The Stop detector has a “wall” design, made of 24 bars 20 mm thick and 120 mm wide. Details of the Stop detector
 83 geometry can be seen on Fig. 4. Further details can be found in Ref. [3].

85 The Stop detector utilises Eljen EJ200 plastic scintillator coupled to XP2020C PMT’s with twisted adiabatic

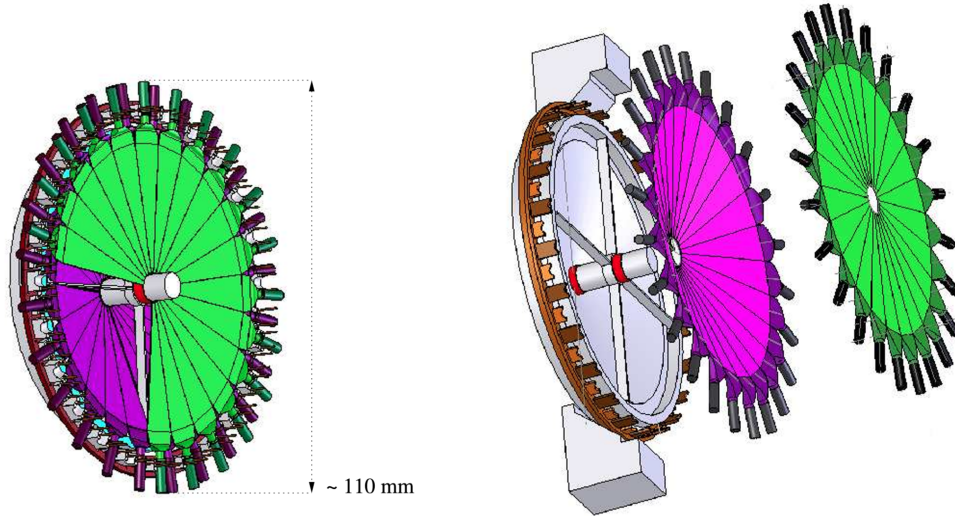


FIG. 3. The Start detector.

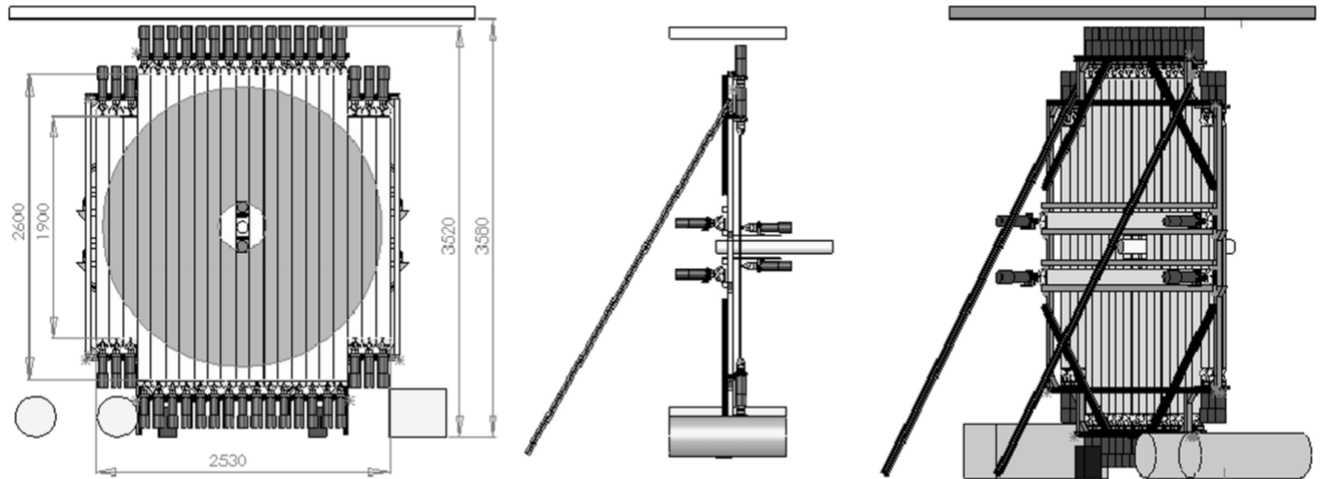


FIG. 4. The Stop detector.

86 lightguides readout from both sides of the bar. All PMT's are housed in 10 mm thick μ -metal housings to minimise
 87 the influence of magnetic field on electron showers. To simplify time calibration, the Stop detector is equipped with
 88 two additional horizontal scintillating bars sitting close to a beampipe, behind the main "wall." Two-side readout
 89 allows to reconstruct hit position along the bar by detectors time difference ($\sigma \sim 3$ cm). However, since position of the
 90 hit will be measured by the tracker right before the wall with much higher accuracy < 1 mm a further improvement
 92 in time resolution is achievable. A KFM tracker will be a four quatro-layered straw tube tracking system, former
 93 WASA-at-COSY FPC. It is composed of 4 identical modules, each with 4 staggered layers of 122 proportional drift
 94 tubes (so called straws) of 8 mm diameter. The design of the detector and the attached electronics is made such as to
 95 preserve the option of charge division readout for obtaining information about the longitudinal hit position along the
 96 sense (anode) wire. Hence, a resistive wire of 35 μ m thick stainless steel is used as the anode wire. The tracker use
 97 50/50 Ar/CO₂ gas mixture and has a 35 μ m position resolution. Further details about FPC can be found in Ref. [4]
 98 and refs within. In original design, 4 modules were arranged as X-Y-V-W planes tilted by 45 degree relative to each
 100 other, see Fig. 6

101 In a KFM design, we plan to arrange modules in two (upstream and downstream) double-layer (X-Y) stations with

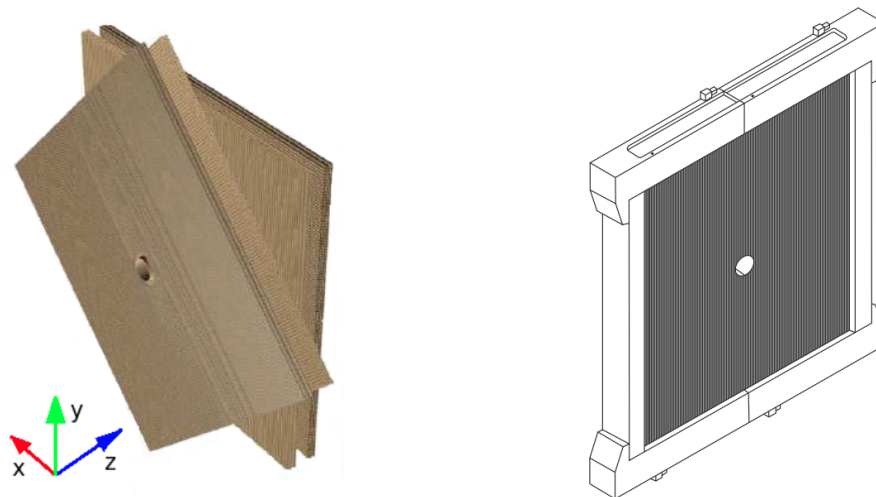


FIG. 5. Schematic view of the tracker. A three dimensional view of four modules of tracker(left) and the single tracker module in a frame(right)

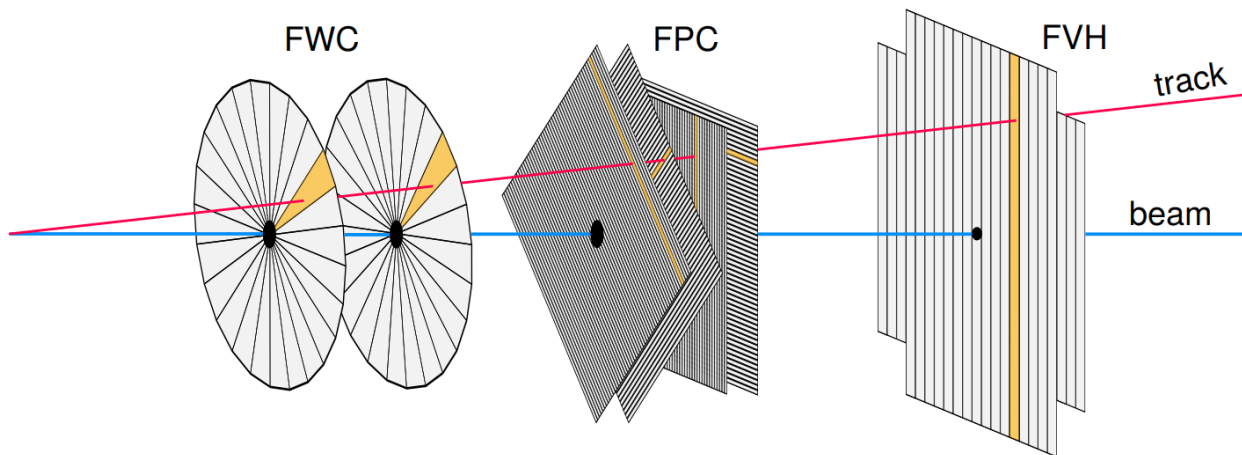


FIG. 6. The original WASA-at-COSY setup of start-stop and tracker systems.

102 2 m distance in between. The upstream one right after the Start detector and downstream one - right before the stop.
 103 This arrangement has two reasons - to increase a level arm and hence increase kaon decay vertex z-position resolution
 104 and to accommodate optional solenoid MRI magnet, Fig. 7.

105 A first implementation of a used MRI machine as a solenoid magnetic spectrometer can probably be traced to
 106 ISOLDE-ISS setup. Indeed, there is a large market of used MRI's where old, but working machines can be accessed at
 107 rather low price. The magnets of old MRI's might be considered rather weak (1.5–3 T) by today's standards, but they
 108 are usually sufficient for scientific purposes. On top of it MRI's are equipped with off-the-shelf shimming as well as very
 109 reliable low maintenance cost cooling systems. All these things make the use of refurbished MRI as a magnetic solenoid
 110 spectrometer very appealing. Magnetic spectrometer is not essential at KFM for kaon flux extraction. However the
 111 use of additional magnetic spectrometer can enhance the programme by accessing physics beyond the standard model
 112 in rare kaon decays and suppressing unwanted backgrounds by additional particle identification abilities of momentum
 113 vs ToF technique. The university of York requested £100k in upcoming grant period 2024–2027 to buy use Siemens
 114 MRI machine and upgrade proposed flux monitor with magnetic spectrometer capabilities. The MRI machines also
 115 have wider bores (70 cm, compare to initially proposed 50 cm KFM magnet bore) which increase KFM acceptance.



FIG. 7. The “optional” used MRI system to be used as a solenoid spectrometer.

116

IV. K_L FLUX DETERMINATION

117 The Kaon flux has a complex dependence on momentum, transverse position and distance from the Be-target. Due
 118 to the $1/z^2$ solid angle suppression (here z is the distance from the Be target), the KFM would see 4 times more kaons
 119 than the LH_2/LD_2 cryogenic target. Also some kaons can decay on the way to the LH_2/LD_2 target within GlueX.
 120 The flux suppression factor due to K_L decay is equal to $f(\beta) = e^{-\frac{z}{c\tau\beta\gamma}}$, where $c = 29.9$ cm/ns is the speed of light,
 121 $\tau = 51$ ns is the K_L mean lifetime; $\beta = v/c$ – kaon velocity in units of speed of light; $\gamma = 1/\sqrt{1 - \beta^2}$. Because of
 122 these dependencies accurate flux monitoring requires determination of the kaon flux as both a function of transversal
 123 position within the beampipe and Kaon energy. A 7 cm beam pipe diameter allows sufficient margins and the clean
 124 definition of a fiducial regions of the transverse beam profile at the KFM position. One should also keep in mind that
 125 the radial extension of the kaon beam varies with kaon momentum – fast kaons tend to be more focused due to the
 126 larger Lorentz boost. All in all, we expect to measure about 4.5k Kaon/s in the KFM. In the Figure. 8, one can see
 127 the Kaon flux experienced by the FM and by the LH_2/LD_2 target respectively. The increased low momentum yield
 128 of Kaons observed in the KFM compared to the target position arises because these low momenta particles have a
 129 larger possibility of decaying in the region between the KFM and a target.

130 To be measured by the kFM, both charged particles from the kaon decay need to be incident within the KFM
 131 acceptance, see Figure 2. Taking into account the different branching ratios, we expect to reconstruct the following
 132 number of K_L from various decay channels, see Figure 9.

133 One can quantify the expected rate in terms of the achievable statistical error within a one day measurement
 134 (Figure 10 left) and the number of days measurement required to get a 1% statistical accuracy in flux (Figure 10
 135 right) for a 20 MeV/c bins in K_L momentum in case of $\pi^+\pi^-\pi^0$ branch analysis.

136 For the kaon beam momenta range appropriate for the hyperon programme a 1% statistical error of the K_L flux
 137 determination is achievable in less than a day. The analysis of a kaon flux described in this section will be performed
 138 offline on a weekly basis with possible daily crosschecks if the online monitoring(described in a section below) would
 139 show any hints for unstable beam behaviour.

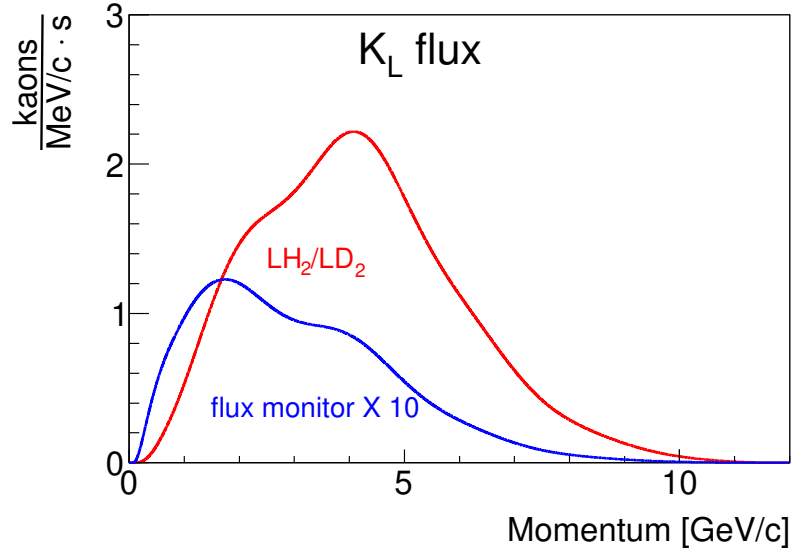


FIG. 8. Kaon flux at LH₂/LD₂ target (red) and at KFM(blue). The yield of events from the KFM is multiplied by 10.

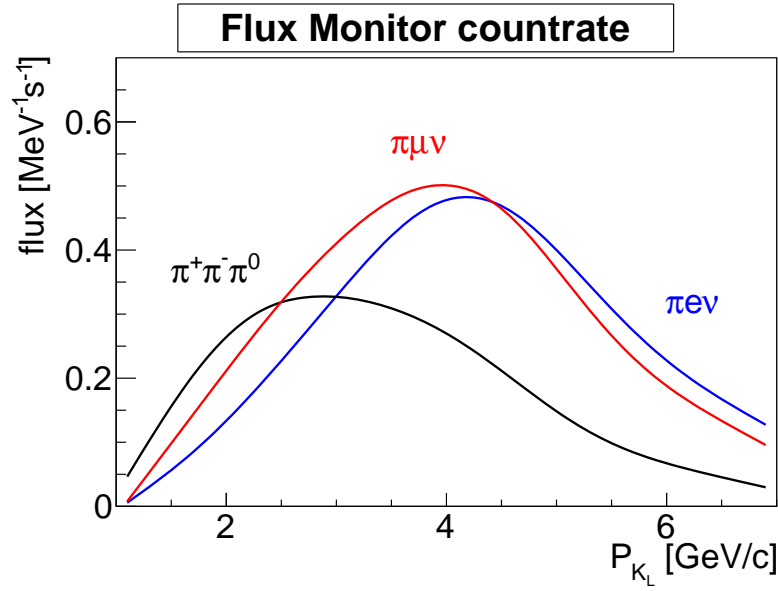


FIG. 9. Visible K_L flux for various decay channels within the FM acceptance.

140

V. VERTEX POSITION RECONSTRUCTION

141 To reconstruct the spatial distribution of the K_L flux within the beam pipe as well as to determine the K_L time-of-
 142 flight from the Be-target, a K_L decay vertex position reconstruction is required. The accuracy of vertex reconstruction
 143 solely depends on accuracy of the tracking modules. With the tracker module described above (the former WASA-
 144 at-COSY FPC), we can achieve the following resolution. In our simulations, we have assumed that both forward and
 145 backward tracking stations are made of X-Y modules with the distance between X and Y layers of 5 cm. The position
 146 accuracy which can be defined from each sub-module is assumed to be $d = 250 \mu\text{m}$. We performed simulations for
 147 both options - the main one (without magnetic field) and an “optional” one with additional MRI solenoid magnetic
 148 field between the stations. The vertex position in the transverse plane is largely defined by the forward tracker,

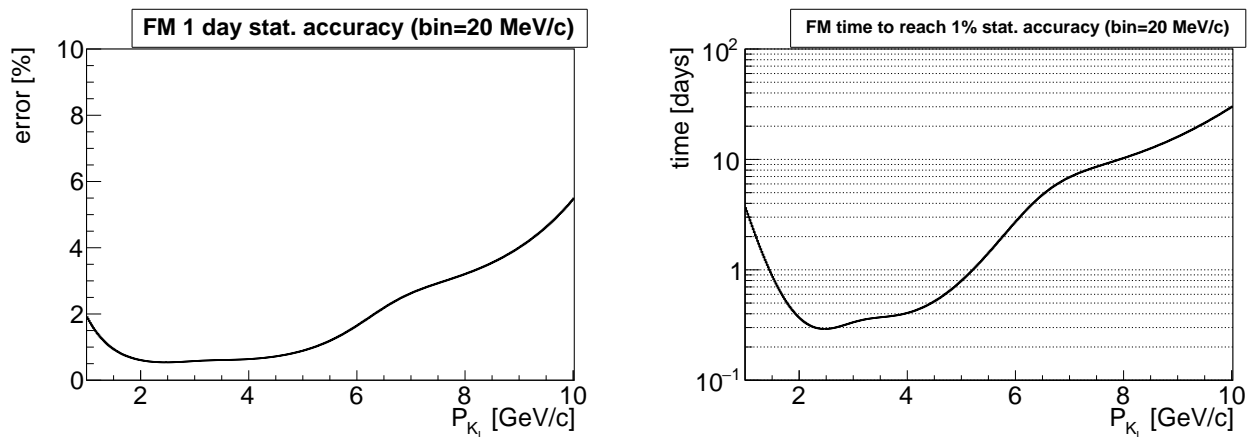


FIG. 10. Expected statistical accuracy for 1 day FM measurement (left) and time to reach 1% accuracy (right) for 20 MeV/c bins in K_L momentum and $\pi^+\pi^-\pi^0$ decay branch.

149 since the magnetic field skews tracks. However, the magnetic field does not change the polar angle (Θ), hence the
 150 position along the beam direction is largely defined by the forward-backward tracker difference. In our resolution
 151 studies we performed a two-track fit, assuming a common vertex, rather than making simultaneous track fits with
 152 vertex extraction from the distance of closest approach of the tracks. In the no-magnetic field mode (ToF mode, main
 153 option) both trackers contribute to the achievable transverse position resolution. The position resolution changes with
 154 distance and polar angle (the closer to the tracker and the higher angle – the better the resolution). On average, one
 155 can say that K_L position resolution in the transverse plane is about $2 \cdot d \sim 0.5$ mm and in the longitudinal direction
 156 $\sim 20 \cdot d \sim 5$ mm, here $d = 250 \mu\text{m}$ is the single plane tracker resolution. Even a $d = 1$ mm tracker resolution should
 157 be tolerable. A typical $250 \mu\text{m}$ resolution which we expect for the KFM tracker would be more than adequate for this
 158 application.

159 VI. DECAY RECONSTRUCTION

160 There are several contributions to a time resolution in current system. The Start detector has a time resolution of
 161 160 ps (including electronics) and has a double-layered design, which can improve the resolution by $\sqrt{2}$. The Stop
 162 detector has somewhat worse time resolution of about 250 ps. Details of the WASA electronics used in the system
 163 can be found in Ref. [7]. The time processing is performed with FastTDC, based on GPX ASIC chip [6] and has
 164 an intrinsic resolution of 81 ps. The K_L decay vertex time resolution defines the achievable momentum resolution.
 165 We expect it to be better than a single track/single cap time resolution, but for our simulations we have assumed
 166 conservative 100 ps [8]. One of the requirement to the KFM time resolution is that it should be better than the
 167 GlueX Start Counter timing due to the 2 times shorter time-of-flight baseline of the KFM compared to GlueX. This
 168 condition can be easily fulfilled with current KFM design.

The momentum resolution in a solenoid magnetic field is fully determined by the tracker resolutions. The displacement in solenoid magnetic field is equal to

$$d' \sim (l^2 \cdot z \cdot 0.3 \cdot B \cdot \sin \Theta) / (2 \cdot p),$$

where l is the length of the magnet [m], B is magnetic field strength [T], z is the particle charge, and p is momentum [GeV/c]. For the $l = B = z = 1$, we have

$$d' \sim (0.3 \cdot \sin \Theta) / (2 \cdot p).$$

169 The Magnetic field only acts on the transversal momentum component. For a typical momentum of 1 GeV/c and a
 170 5 degree polar angle a displacement of 13 mm is expected. For a 1 GeV/c and 1 degree polar angle a displacement
 171 would be the reduced to 2.6 mm (With a standard MRI $z = 1.8$ m and $B = 1.5$ T corresponding numbers would be
 172 64 mm and 13 mm). Despite these deficiencies a magnetic field momentum reconstruction is expected to work a lot
 173 better than the ToF reconstruction. The expected performance of ToF and magnetic reconstruction is illustrated in
 174 Figure 11.

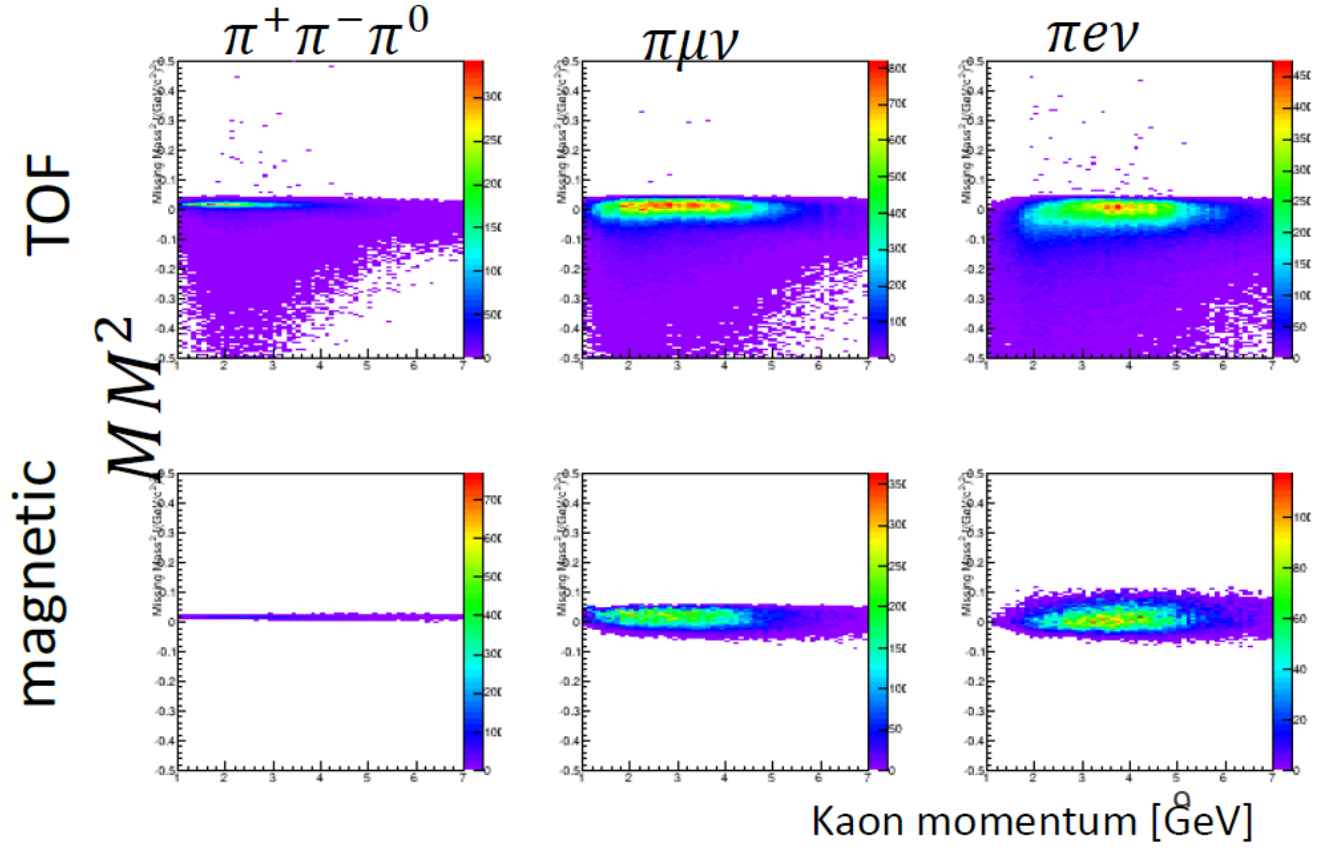


FIG. 11. Missing mass reconstruction with ToF and magnet as a function of kaon momentum. All charged particles in all decay channels are assumed to have mass of pion.

175 Correct mass assignment for the $\pi^+\pi^-\pi^0$ branch give a much narrower Missing Mass (MM) distribution. A 1-
 176 Dimensional projection to the y-axis, as shown in Figure 12 allows a direct comparison of various case scenarios.

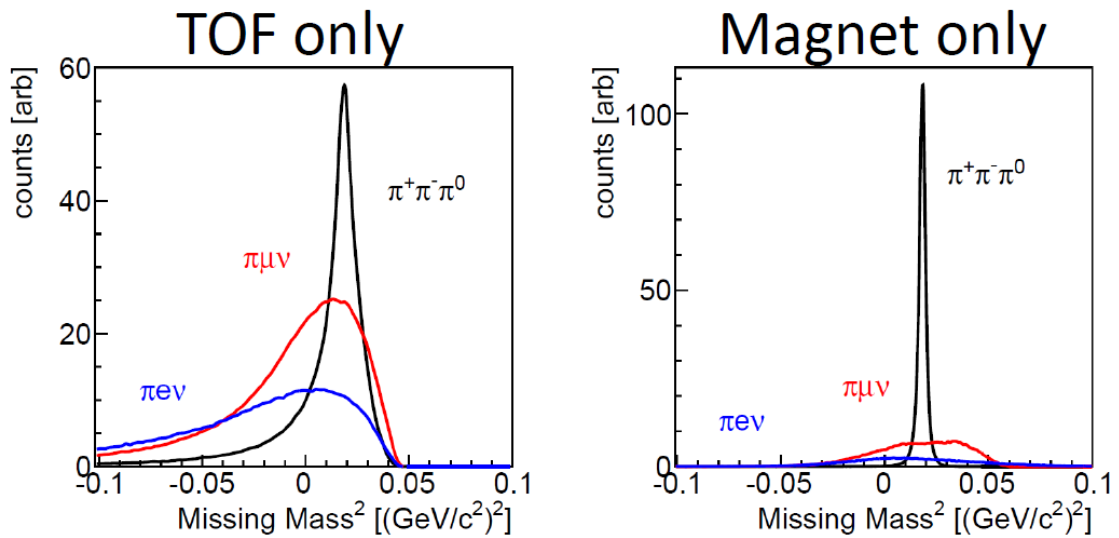


FIG. 12. Missing mass squared for the ToF and magnetic reconstruction of kaon decay.

177 Since the ratio between different branches is known extremely well, in absence of background ToF reconstruction is
 178 sufficient. In the presence of unknown background an additional rejection condition or particle identification technique
 179 β/p might be useful. As expected, the magnetic field provides more precise event reconstruction.

180 A. Background

181 One of the essential conditions for the KFM was the absence of the KLF induced background on the main GlueX
 182 spectrometer. In particular there were concerns that KLF magnetic system may guide charged particles into a GlueX
 183 tracker. We have studied various aspects if a solenoidal magnetic field can induce additional background and if a
 184 dipole magnetic field from the pair spectrometer magnet, which in our design is used as a swiping magnet can enhance
 185 a background. It was found that the answer on both questions is No! A solenoidal magnetic field does not change
 186 the background at all. A presence of an MRI machine slightly reduces the background since it is served as a passive
 187 shielding. The pair spectrometer magnet, when operational, marginally decreases the level of the background by
 188 swiping away some charged particles which otherwise might end up in a GlueX spectrometer. In general, the influence
 189 of KFM on a GlueX background conditions is very small, which is dominated by kaons decayed further downstream.

190 VII. NEUTRON BACKGROUND

191 We do not expect any influence of a neutron background on the KFM. A similar system of ToF scintillators with
 192 trackers was working at the WASA detector for a decade under several orders of magnitude higher neutron fluxes
 193 without showing signal deterioration. Conventional PMT's proved to be very tolerable to a neutron flux. We also do
 194 not expect any neutron flux mediated disturbances in kaon flux measurements. At the position of the KFM assembly
 195 the neutron flux is more or less confined within the beam pipe. However, the divergence of a neutron beam will
 196 cause some charge particle background, which would be seen by the KFM. In some cases, like two-proton knockout or
 197 $nn \rightarrow pn\pi^-$ reactions in the beam pipe material these events might mimic kaon decays. Fortunately, all these events
 198 would originate from the beampipe with a vertex displacement of a 35 mm in transversal direction, allowing a fair
 199 separation from useful kaon decays. The KFM tracker system will provide sufficient accuracy to disentangle these
 200 cases with simple fiducial cuts. One also needs to take into account that kaons and neutrons are largely separated in
 201 time, see Figure 13. Neutron in tails from previous bunches are too slow to produce two charge tracks reactions which
 202 can be misidentified with kaons. So in reality we need to care about a lot less neutrons which have similar velocities
 203 to kaons but with vertex reconstruction and missing mass determination such events can be eliminated.

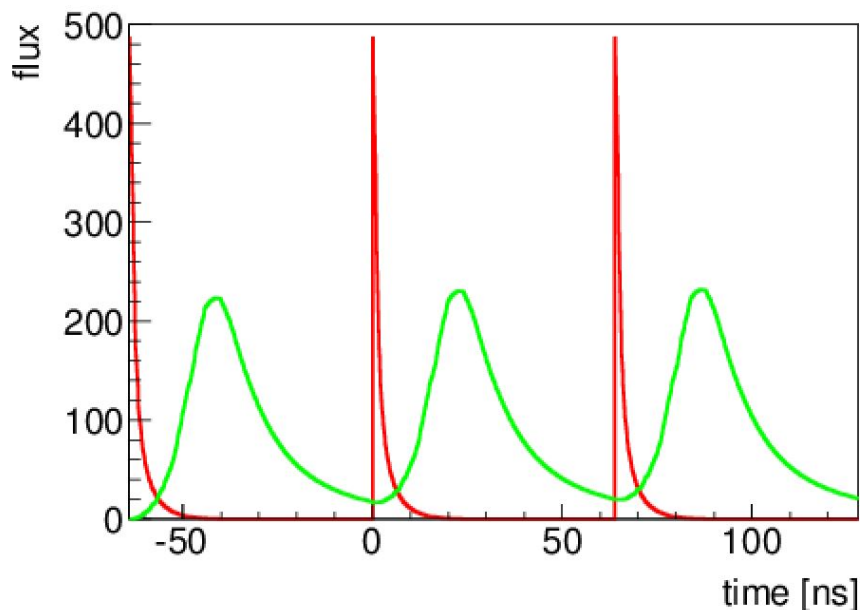


FIG. 13. Time structure of kaon (red) and neutron (green) fluxes.

VIII. ONLINE MONITORING

Kaon beam is produced in a two-step process ($e^- \rightarrow \gamma \rightarrow K_L$) with extremely large level arms between production stations. That is why it is absolutely mandatory to monitor both position and momentum distribution of kaon flux online to adjust electron beam properties when necessary.

Due to reasonably low count rate, we expect to perform a full event reconstruction online in event-by-event basis. In addition, we also plan to perform a “simplified” monitoring which would not require the full reconstruction and accurate calibration to get the basic information. Due to cylindrical symmetry of a KFM start detector we expect uniform count rate over all elements. However, if a kaon beam would get some misalignment, we expect to see it immediately on a start counter detector rate.

A rough kaon momentum monitoring also do not require precise event reconstruction. Without tracking information the precise knowledge about kaon decay vertex is unavailable. However, we still know that it happen somewhere within 2 meters between the centre of the pair spectrometer magnet and a start detector. In a simplified monitoring routine we can assume that kaon decayed at location of start detector and that kaon time of flight is defined as a time difference between photon arrival time to a Be-target and an average time of two hits of start detector. Under these assumptions, we will get a following momentum resolution uncertainty, see Fig. 14(averaged over three 2-charged track decay channels).

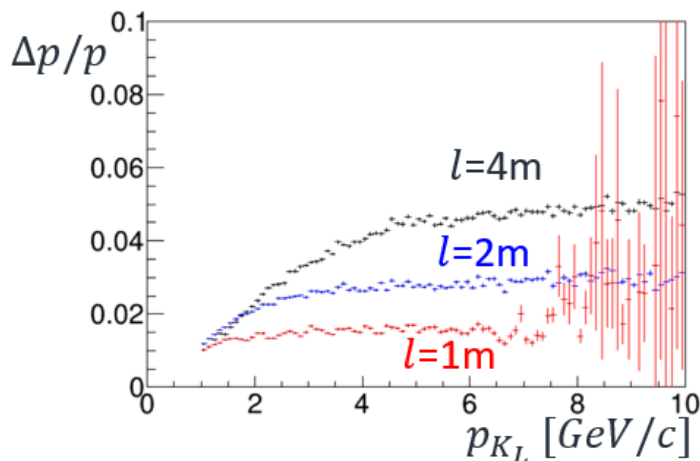


FIG. 14. Accuracy of simplified kaon momentum reconstruction without tracker. The length l correspond to a distance between the centre of pair spectrometer magnet and a Start detector.

A decent accuracy of $\sim 3\%$ is achievable with proper calibration. However, since accounting for the light propagation time in the detector elements require tracking, an achievable time resolution will be a bit worse - 5–10%. Which is still sufficient for the online monitoring and beam adjustments.

A monitoring of a neutron flux is a challenging task, especially if an accurate absolute normalisation is required. A neutron flux, seen by the cryo target might also provide useful information about the beam quality. To have rough relative monitoring of neutrons, we plan to install a 10 cm plastic scintillator block ($\sim 1\%$ detection rate for neutrons above $E_n \sim 100$ MeV) in front of a beam dump reading its rate as a scaler.

IX. EXISTING EQUIPMENT AND RELOCATION TIMELINE

As described above, in a benchmark design the KFM will consist of a time-of-flight system (KFM-TOF) and a tracker (KFMPC). Both parts of equipment re-utilise existing components of the WASA-at-COSY detectors. The KFM-TOF consist of two detectors - a Start detector (Forward Window Counter) and a Stop detector (Forward Veto hodoscope) designed and constructed at the University of Tübingen, Germany (PI - H. Clement and Co-PI - M. Bashkanov). A tracker was constructed at the University of Uppsala, Sweden (PI - T. Johansson). Currently both detectors are still installed at the COSY (Jülich, Germany) and will be available for relocation from Q4 2023. It was agreed with both university PIs and a Jülich research centre that these detectors and associated equipment can be

235 used at KLF. Both detector system have dimensions (beam pipe hole diameter, distance from the beam pipe to the
 236 floor, active detector diameter) which fits KFM design very well and do not require any further modifications.

237

X. DECOMMISSIONING

238 Due to very small particle fluxes we expect negligible level of KFM activation, which should allow KFM decom-
 239 missioning more or less immediately after the end of a beamtime. Removing of all KFM detector components is
 240 straightforward end expected to be done in less than a month time. An reverse installation of a pair spectrometer
 241 and a shielding wall will require another month, since also a beamline needs to be reversed as well.

242

XI. COSTS

243 The University of York as a KFM PI requested £22k from upcoming UKRI consolidated grant (2024–2027) for
 244 relocation and commissioning of these systems (This comprises relocation (£10k), construction and commissioning
 245 of a new support system (£5k) and making a new readout DAQ[new DAQ computer + communication electronic]
 246 (£7k)). We have also requested 40% FTE PDRA to perform this relocation and 20% FTE technician.

247 Besides measuring kaon flux, KFM may significantly contribute to study of rare and CP-violating K_L -decays. One
 248 of the most rarest, $Br \sim 10^{-9}$ K_L β -decay, will be unique mode which can be accessed at KFM. To enable this
 249 optional part of the program we further requested (£100k) for purchasing an ex-MRI magnet (£85k) which will suffice
 250 to provide the solenoid magnetic field. We also requested shipping costs (£15k) and associated technical/PDRA
 251 support during its installation. We already got very positive responses from grant panel reviewers, however the final
 252 decision, including funding allocation, is pending.

253

XII. JLAB CONTRIBUTION

254 It is expected that JLab will provide cooling water (~ 40 l/min to 120 l/min) for the magnet, electricity (~ 15 kW)
 255 and organise mounting points for the newly coming equipment. According to JLab engineering stuff all these additions
 256 are easily manageable.

257 No modifications of the platform is necessary in both magnet and no-magnet design. A replacement of a photon
 258 beamline to accommodate larger diameter of the kaon beam is foreseen. The only two requirement from a KFM side
 259 - the use of low permeability stainless steel for the pipe to accommodate magnet design and the use of dedicated
 260 section with two flanges to simplify KFM installations are incorporated in the engineering drawing.

261

XIII. SUMMARY

262 The K_L flux determination with proposed Flux Monitor and accuracy better than 5% over the full range of energies
 263 seems to be feasible. The construction is straightforward and can be completed within 1 year. No prototyping is
 264 necessary. The achievable reconstruction resolution is determined by the tracking system and TDC electronics. The
 265 overall cost of the KFM construction is very low. No interference with existing Hall-D equipment is expected.

XIV. APPENDIX A: CAD DRAWINGS

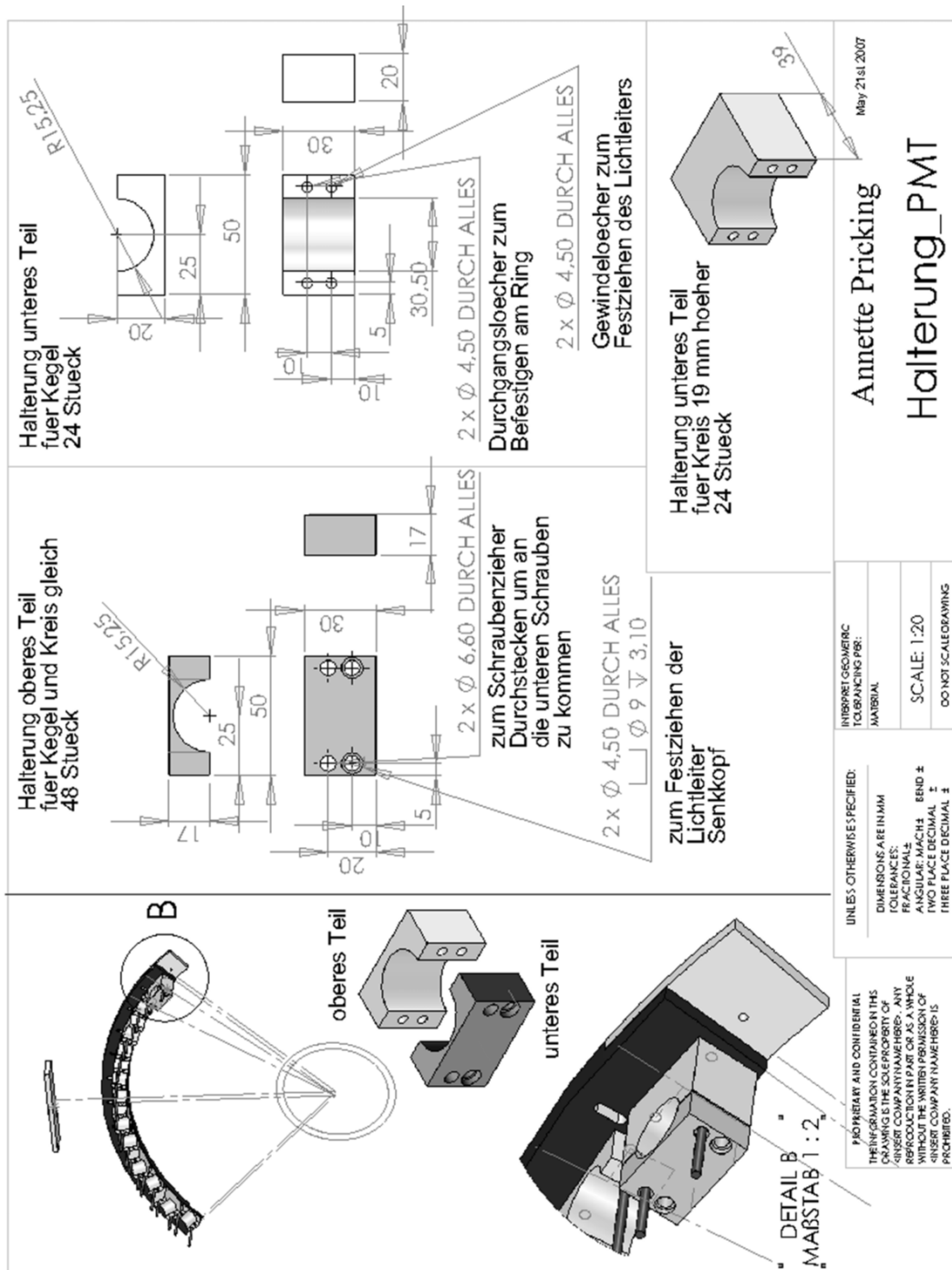


FIG. 15. Start detector mounting system CAD Drawing.

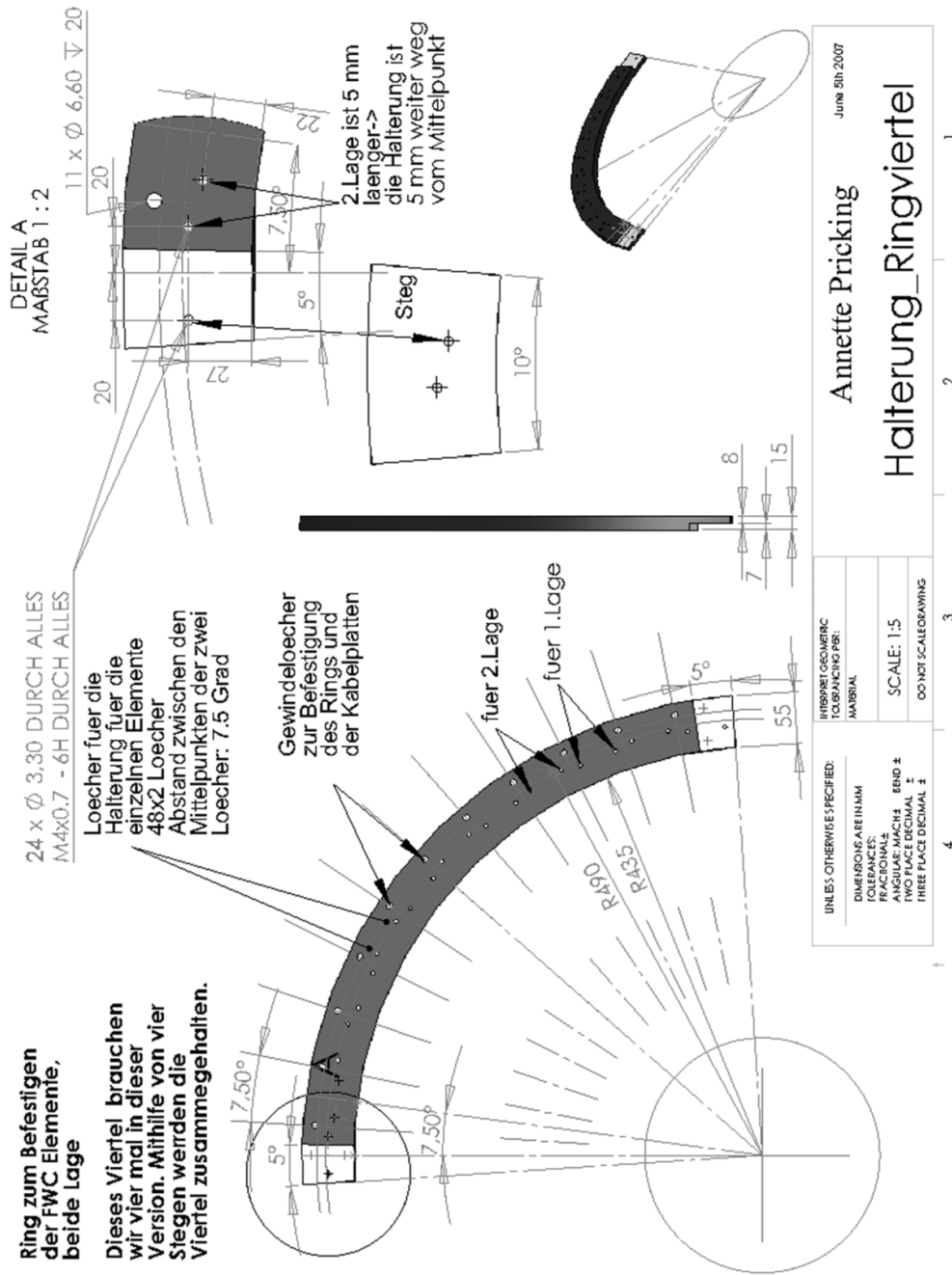


FIG. 16. Start detector support CAD Drawing.

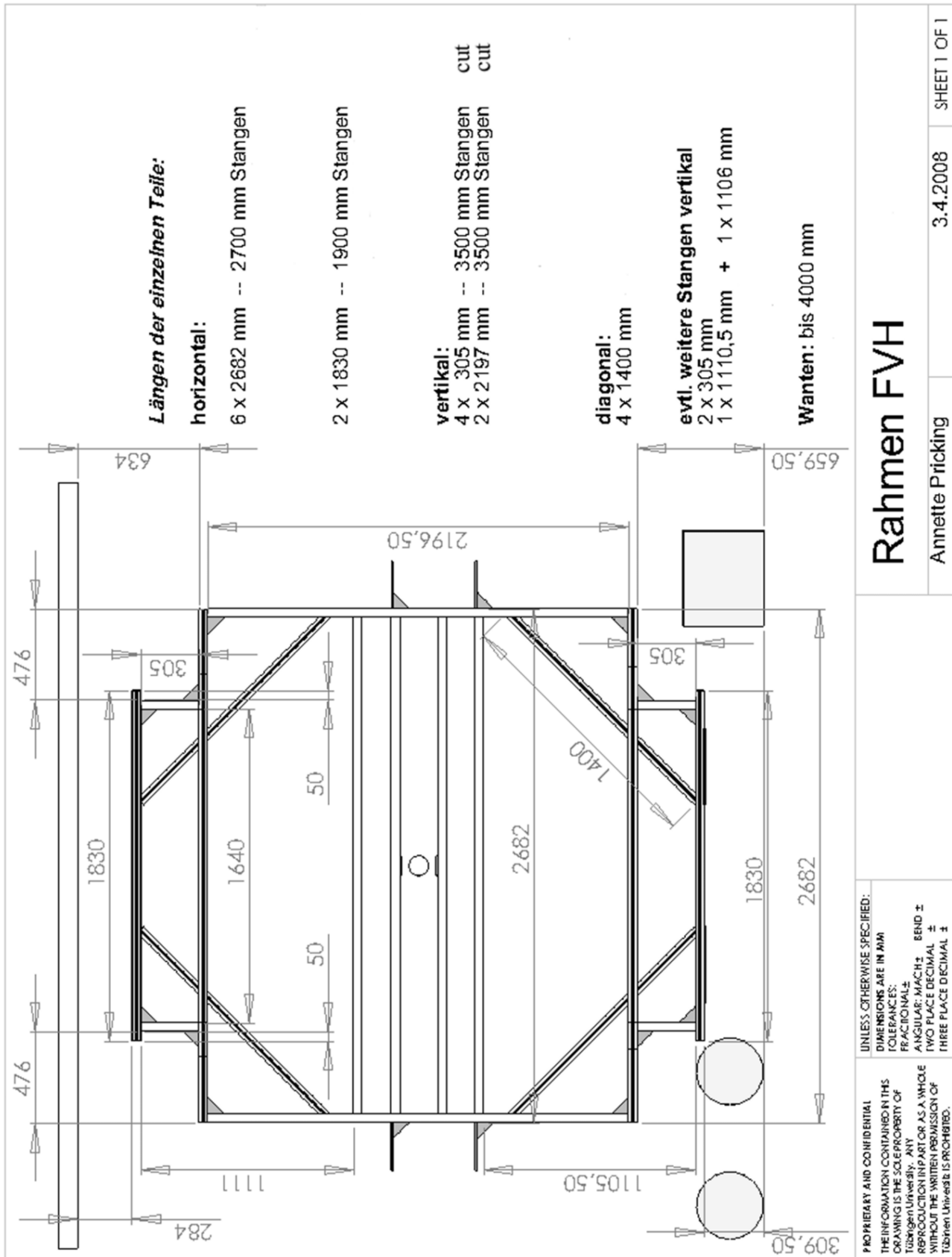


FIG. 17. Stop detector support structure CAD Drawing.

-
- 267 [1] M. G. Albrow, D. Aston, D. P. Barber, L. Bird, R. J. Ellison, C. Halliwell, A. E. Harckham, F. K. Loebinger, P. G. Murphy,
268 J. Walters *et al.* “Photoproduction of k_0 mesons from protons and from complex nuclei,” Nucl. Phys. B **23**, 509 (1970).
- 269 [2] R. L. Workman *et al.* [Particle Data Group], “Review of Particle Physics,” PTEP **2022**, 083C01 (2022).
- 270 [3] A. Prcking, “Double pionic fusion to ^4He ,” Ph.D. Thesis, Tübingen Univ., (2010); [https://publikationen.uni-](https://publikationen.uni-tuebingen.de/xmlui/handle/10900/49542)
271 [tuebingen.de/xmlui/handle/10900/49542](https://publikationen.uni-tuebingen.de/xmlui/handle/10900/49542) .
- 272 [4] H. H. Adam *et al.* [WASA-at-COSY Collaboration], “Proposal for the wide angle shower apparatus (WASA) at COSY-Jülich:
273 WASA at COSY,” [arXiv:nucl-ex/0411038 [nucl-ex]].
- 274 [5] H. Kleines *et al.* “Development of a high resolution TDC module for the WASA detector system based on the GPX ASIC.,”
275 IEEE Nucl. Sci. Symposium Conf. Record, **30**, 1005 (2006).
- 276 [6] TDC-GPX Datasheet. Acam Messelectronic GMBH, 2006.
- 277 [7] H. Kleines, K. Zvoll, P. Wustner, W. Erven, P. Kammerling, G. Kemmerling, H. W. Loevenich, A. Ackens, M. Wolke,
278 V. Hejny *et al.* “The new DAQ system for WASA-at-COSY,” IEEE Trans. Nucl. Sci. **53**, 893 (2006).
- 279 [8] Each event has 8 time stamps 4 from Start detector and 4 from Stop one due to 2 charged track geometry.